Reference: *Biol. Bull.* **182**: 66–76. (February, 1992)

Isolation of Neurons of a Nudibranch Veliger

FU-SHIANG CHIA, RON KOSS, SHAUNA STEVENS, AND JEFF I. GOLDBERG

Department of Zoology, University of Alberta, Edmonton, Alberta, Canada T6G 2E9

Abstract. A technique was developed to dissociate and culture identified sensory neurons and interneurons from the anterolateral propodial ganglia of metamorphically competent veligers of the nudibranch, *Onchidoris bilamellata*. Receptor cells have been represented as receiving an environmental cue that initiates the settlement response. The ganglionic cells, along with other cell-types from the propodial region housing the ganglia, were excised with a large-bore micropipette, and dissociated by mild trypsin incubation and trituration. Cells and tissues were plated in poly-L-lysine-coated plastic culture dishes containing modified *Aplysia* medium and survived for up to four days. The different cell-types possess diagnostic features, so they can be recognized under culture conditions. Sensory cells were bipolar in profile, with one end of the cell being thickened, representing the receptor apparatus. Interneurons are unipolar or bipolar in shape, and bear thin neurites. Other cell-types, including myocytes, ciliated epidermal cells, nonciliated epidermal cells, and gland cells were identified. Identifications of living cells were corroborated through electron microscopical analysis.

Introduction

The propodium of the advanced veliger larva of the nudibranch *Onchidoris bilamellata* contains a unique set of morphologically identifiable structures called the anterolateral ganglia (Chia and Koss, 1989). These structures are thought to be involved in perception of the environmental cues that induce settlement and metamorphosis (Chia and Koss, 1988). Recently, it has been shown that sensory receptor cells within the anterolateral ganglia respond to a known settlement cue (barnacle-conditioned seawater) by producing slow, low-amplitude depolarizations that can be detected by the application of conventional intracellular recording methods (Arkett *et al.*, 1989). However, the activity of the sensory cells is variable in terms of duration and amplitude. Such variability may be due to the changeable concentration of crude stimulus being administered, the developmental status of the receptors, or the degree of damage caused by the electrode upon entry into the cell. Also unclear is the depth within the ganglion that the electrode was placed, and whether the epidermal tissues overlying these subepidermal structures altered the response of receptor cells.

In this paper we report a technique for excising, dissociating, and culturing the lateral propodial region of the veliger foot of *O. bilamellata*. This work was undertaken with a view to studying the responses of the isolated cells to settlement or metamorphic cues, thereby overcoming many of the limitations presented by the intact preparation.

Received 10 September 1990; accepted 25 November 1991.

Materials and Methods

Egg ribbons from *Onchidoris bilamellata* (Linnaeus, 1767) were collected at Bamfield Marine Station, Bamfield, British Columbia, Canada, and transported to the University of Alberta. Veliger larvae were then raised according to the method of Chia and Koss (1988). The veligers used in these experiments were from the same cohort, and random samples from the cohort were checked for metamorphic competency according to Chia and Koss (1988).

Veligers were pipetted into a Sylgard (Dow Corning)-lined dish containing 2.5 ml of a high Mg^{++}, low Ca^{++} seawater mixture (12–15°C) consisting of natural seawater, isotonic (0.33 *M*) $MgCl_2$, and Co^{++}-seawater in a ratio of 2:1:4.5 (v/v/v). Co^{++}-seawater consisted of 430 m*M* NaCl, 10 m*M* $CoCl_2$, 10 m*M* KCl, 30 m*M* $MgCl_2$, 20 m*M* $MgSO_4$, 10 m*M* TES pH 7.8 (Arkett *et al.*, 1987, 1989). Veligers were tethered with a cactus spine, which was inserted through the base of the velum. A second

spine was placed through the tip of the foot, and a third spine was used to orient the veliger such that one side of the propodium and receptor field faced upward (Figs. 1, 2).

Larvae were subsequently incubated for 5 min in 0.2% trypsin (Sigma) in an *Aplysia* defined medium [mADM: 50% Liebowitz L-15 (Gibco special order); 0.26 *M* NaCl; 9.7 m*M* $CaCl_2$; 4.6 m*M* KCl; 26 m*M* $MgSO_4$; 26 m*M* $MgCl_2$; 2 m*M* $NaHCO_3$; 33 m*M* Dextrose; 10 m*M* Hepes; 0.015% L-glutamine; 50 μg per ml gentamicin] modified from Schacher and Proshansky (1983). This solution was eventually replaced with mADM.

The anterolateral ganglion, which is visible as an oblong cellular mass, was located using a dissecting microscope, and a silicon-coated (Sigmacoat) micropipette, with a bore diameter of 20–30 μm, was placed directly on it. A micromanipulator was used to place the micropipette. The tissue was excised by first applying mechanical force with the micropipette to this region, and then alternating negative and positive pressure within the micropipette through a microsuction device (Canlab). The excised tissues, including the portions of the anterolateral ganglion and propodial epidermis, were triturated in the micropipette. The dissociated cells were then plated on to high molecular weight poly-L-lysine (Sigma) coated plastic 35 mm tissue culture plates (Falcon) in cold mADM. The cultures were maintained at 4°C for 24 to 72 h.

Cell cultures were viewed and photographed live with a Nikon TMD inverted photomicroscope equipped with phase-contrast optics. Cultures to be fixed for transmission electron microscopy (TEM) were stained with Richardson's stain (Richardson *et al.*, 1960) to locate the cells in the culture dish. For TEM, cells were fixed for 1 h in 2.5% glutaraldehyde in 0.2 *M* phosphate buffer (pH 7.6), followed by a 1 h post-fixation in 2% OsO_4 in 1.25% sodium bicarbonate (pH 7.2, Wood and Luft, 1965). They were then dehydrated through an ethanol series, and directly embedded in Medcast (Ted Pella Inc.). After a polymerization period of 72 h, the Medcast was peeled from the culture dish, mounted on Medcast blanks with Krazy Glue, and sectioned with a diamond knife. Sections were stained with uranyl acetate and lead citrate (10 min each). Sections were examined with a Philips E. M. 201 electron microscope.

For scanning electron microscopy (SEM), larvae were relaxed in the Co^{++}-seawater mixture described above, and processed according to the technique of McEuen (1985). Specimens were then examined with a Cambridge Stereoscan 250 SEM.

Results

The foot of the advanced veliger of *O. bilamellata* is a large structure consisting of a metapodium and propodium (Figs. 1, 2). In veligers that have been immobilized in the high Mg^{++}, low Ca^{++} seawater, the location of each anterolateral ganglion is evident as an oblong, cilia-free region on the foremost sides of the propodium (Fig. 2). The sensory fields overlying the anterolateral ganglia are composed of a mosaic of cell-types including the dendrites of sensory cells, epidermal cells, multicellular metapodial glands, and muscle cells (Figs. 3–5). Some untargeted tissues and cells were inevitably excised along with the target tissues, and will be characterized because they are present in cultures of dissociated cells.

The pair of anterolateral propodial ganglia are located below the level of the epidermis (Figs. 3, 5). They are oblong structures, consisting of an outer cortex of cell bodies and an inner neuropil of fibers (Chia and Koss, 1989). The cell-types constituting the cortex include sensory cells, neurons, and sheath cells; neurons occupy the inner layer adjacent to the neuropil, while sensory cells are more numerous and distributed around the outer, lateral perimeter of each ganglion. Bundles of dendritic processes originating from sensory cells traverse the epidermis to form the external sensory fields mentioned above (Figs. 1, 2, 5). Sheath cells encapsulate the ganglia. The anterolateral ganglia are connected to the central nervous system, *i.e.*, cerebral ganglia, by short commissures.

After excision of a ganglion, the dissociated cells settled within 24 h of plating. Cells settled in clusters or as individuals and attached to the substratum. Several cell-types were identifiable at the level of the light microscope on the basis of their size and morphology. These included: epidermal cells (both ciliated and nonciliated), gland cells, muscle cells, neurons, and sensory neurons (Figs. 7, 10, 13, 16, 19, 22, 25, 29). The appearance of these cells was constant in several separate dissociations and was comparable to those identified by *in situ* study. Most importantly, the fine structure of the different cell-types *in situ* was conserved under *in vitro* conditions, thus corroborating the identification of cell-types according to light microscopy.

Epidermal cells

In its natural state, the epidermis covering the anterolateral ganglion is composed primarily of multiciliated cells and cells with long branched microvilli projecting from their apices (Figs. 5, 6, 9). Both cell-types are cuboidal in profile and attach to the basal lamina through a hemidesmosome complex involving numerous microfilaments. Those cells that bear microvilli contain numerous mitochondria within the apical portion of the cell; electron-dense granules of about 0.2 μm in diameter are found immediately below these organelles (Fig. 6). Multiciliated cells also possess numerous distal mitochondria, which

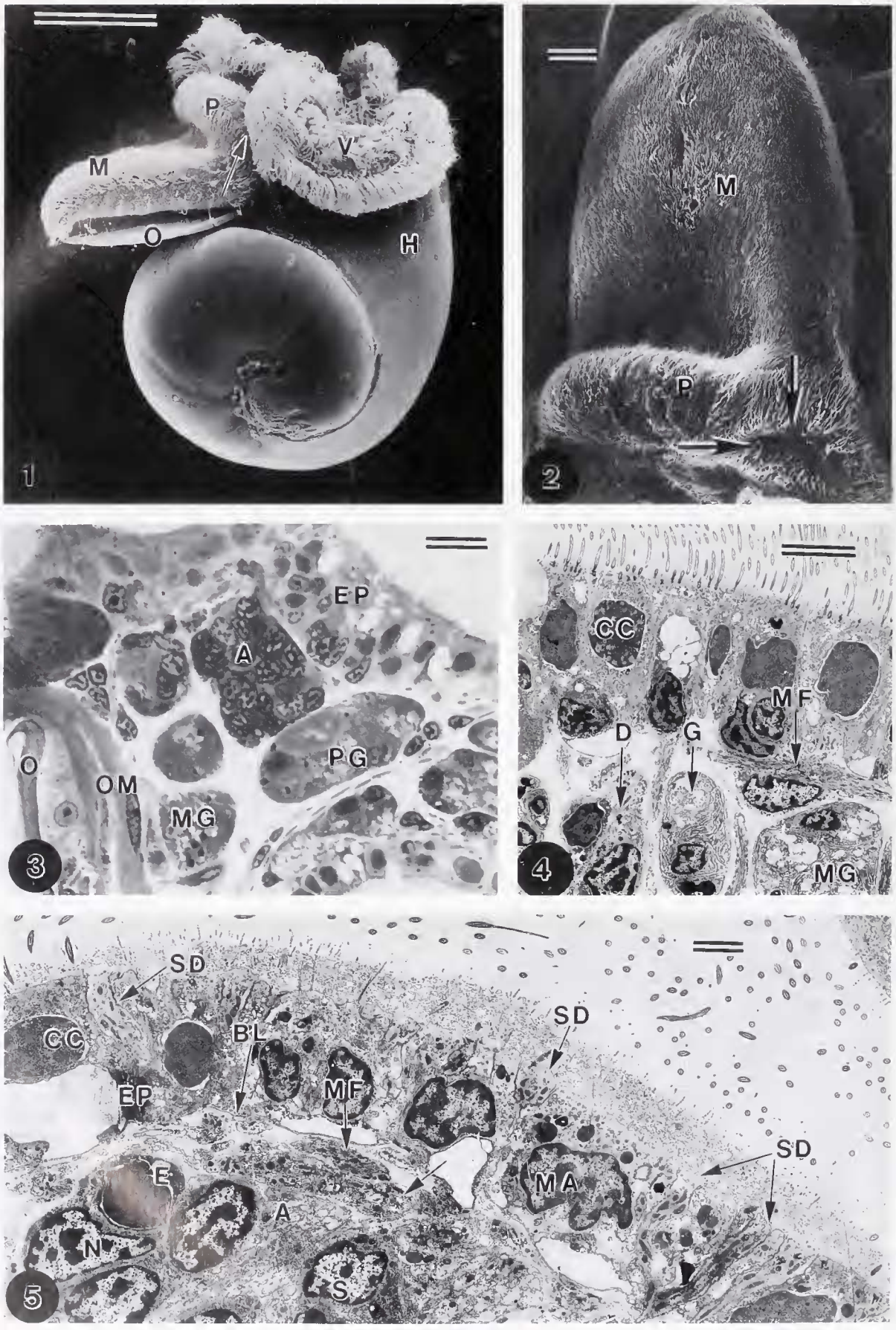
P
V
M
O
H
1
M
P
2
EP
A
PG
O
OM
MG
3
CC
MF
D
G
4
MG
SD
CC
BL
SD
EP
MF
SD
E
MA
A
N
S
5

are distributed among the ciliary rootlets. Nuclei occupy the basal regions of both cell-types. However, the cytoplasm and the nuclei of microvillar cells stain less densely than ciliated cells, while the latter possess unique vacuoles with electron-translucent contents.

Immediately after dissociation of a ganglion, cultures are dominated by ciliated and non-ciliated epidermal cells, many of which fail to attach to the poly-L-lysine substratum. Ciliated and nonciliated epidermal cells were readily recognizable at the light microscopy level because both types of cell were round (Figs. 7, 10). In ciliated cells, the cilia were readily identifiable (Fig. 10). After trituration, both of these types of cell generally remained aggregated. The structural characteristics of the *in situ* and *in vitro* ciliated and nonciliated epidermal cells are similar; those cells found in culture are round to cuboidal and contain microfilaments, numerous mitochondria, and microvilli or cilia (Figs. 5, 6, 8, 9, 11). The substructure of the cilium includes a ciliary rootlet. Within a day, cilia appear to be reabsorbed into the cell. In contrast, nonciliated epidermal cells contain characteristic electron-opaque granules of about 0.5 μm in diameter, and the nucleus stains lightly.

Muscle cells

Muscle cells are numerous throughout the propodium and lie adjacent or attach to the basal lamina. They are filamentous in profile and their contents are dominated by myofilaments (Figs. 3, 4, 12). Mitochondria are scattered around a centrally positioned elliptical nucleus, which is displaced away from the main stream of myofilaments (Fig. 12). Individual muscle cells found under culture conditions are identical in shape and structure. They are large and filamentous in appearance and their nucleus protrudes from one side of the cell (Figs. 13, 14). The cytoplasm contains bundles of myofilaments which extend the length of the cell, and mitochondria which are scattered around the nucleus (Fig. 14).

Secretory cells

The metapodial glands of intact ganglia are flask-shaped structures and are located below the level of the epidermis (Figs. 3–5). They contain two types of gland cells (Figs. 4, 15, 18). The first, or type A secretory cell, contains inclusions that are composed of flocculent material; free ribosomes and rough endoplasmic reticulum are dominant organelles and surround an oblong nucleus (Fig. 15). The second, or type B secretory cell has a densely staining nucleus, and its cytoplasm is filled with small electron-dense granules averaging 0.1 μm in diameter (Fig. 18). Isolated metapodial gland secretory cells had the same overall morphology; they were large and bulbous, with the nucleus occupying the rounded end of the cell (Figs. 15, 17, 18, 20). In certain instances, large secretory vacuoles in type A cells gave the interior of the cell a convoluted appearance when observed by light microscopy. Isolated type A secretory cells contained the vacuoles and extensive rough endoplasmic reticulum observed *in situ* (Fig. 17). Cultured type B cells contained the electron-dense granules present *in situ* and could often be distinguished from type A cells by their smaller cytoplasmic protrusions (Fig. 20).

Ganglionic cells

Anterolateral ganglia are composed of sheath cells, neurons (Figs. 21, 24), and sensory receptor cells (Figs. 27, 28) whose configuration, distribution, and fine structure have been described in detail by Chia and Koss (1989). Sheath cells stain densely and encapsulate the anterolateral ganglia through long, slender processes. How-

Figure 1. Scanning electron micrograph (SEM) of an advanced veliger showing location of one of the pair of settlement receptor fields (arrow), propodium (P), metapodium (M), shell (H), velum (V), and operculum (O). Bar = 100 μm.

Figure 2. Higher magnification SEM showing a receptor field (arrows) and the foot with propodium (P) and metapodium (M). Bar = 20 μm.

Figure 3. Section (1 μm thickness) through the propodium identifying the position of the anterolateral ganglia (A), covering epidermis (EP), operculum (O), and opercular muscle (OM). The multilobular propodial glands (PG) and the smaller metapodial glands (MG) are also shown. Bar = 10 μm.

Figure 4. Transmission electron micrograph of section through a ciliated region of the propodium showing the epidermis composed of ciliated cells (CC), overlying metapodial glands (MG), and muscle cells and fibers (MF). Note that the secretory cells within the metapodial glands are of two types; one type has large electron-translucent inclusions (G) and the other type has darkly staining nuclei and small electron-dense granules (D). Bar = 5 μm.

Figure 5. Cross section through the lateral propodial region showing that the anterolateral ganglion (A) is composed of sensory cells (S) with radiating ciliated dendritic endings (SD), interneurons (N), and sheath cells (E). The epidermis (EP) contains ciliated cells (CC), microvillar cells (MA) with elongate microvilli, and the ramifications of sensory cell terminals. Also note the basal lamina (BL), muscle cell (MF) and metapodial gland cell processes (arrow). Bar = 2.5 μm.

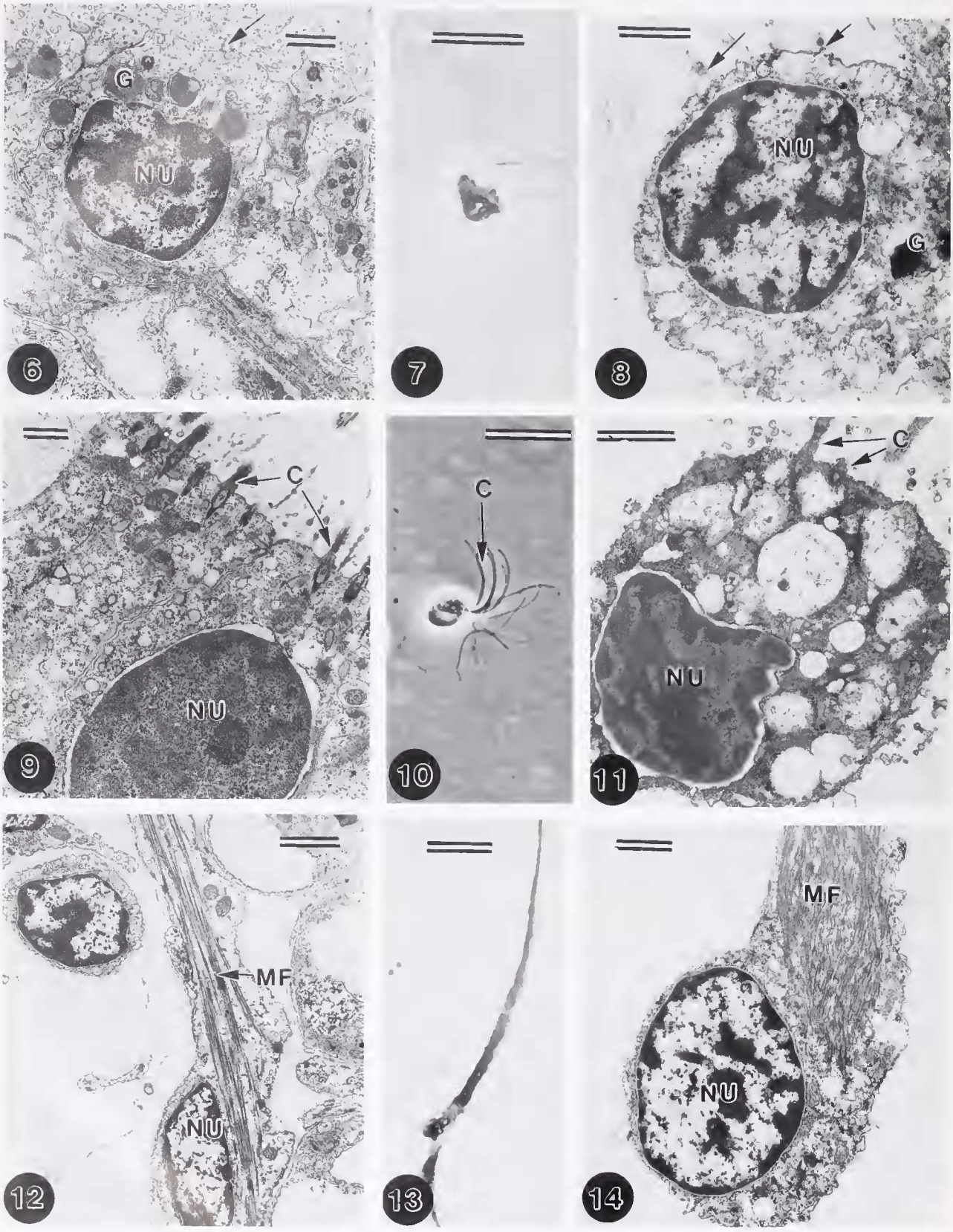

Figure 6. Section through an *in situ* microvillus cell located in the epidermis overlying the anterolateral ganglion. Note the nucleus (NU), electron-dense granules (G) and microvilli (arrow). Bar = 1 μm.

Figure 7. Phase-contrast photomicrograph of a cultured microvillus cell isolated from the lateral propodial region of a competent *Onchidoris* veliger. Bar = 10 μm.

ever, isolated sheath cells were never found in cultures of dissociated cells, although they were rarely observed attached to undissociated clusters of neurons and sensory cells.

Neurons are located deep within an intact ganglion. Their cell bodies contain a relatively clear cytoplasm, a lightly staining nucleus, free ribosomes, and a small number of vesicles (Figs. 21, 24). They possess one or two thin neurites, which, depending upon the location of that neuron within the ganglion, projected from the cell body (Fig. 24) into the neuropil or the commissure that connects to the cerebral ganglion. *In situ* neurites are visualized as thin processes that contain a few vesicles, microtubules, and the occasional mitochondrion (Fig. 24); neurons do not communicate with the external environment and do not possess cilia.

Neurons plated from the anterolateral ganglion were identified by the presence of long thin, sometimes branched processes that extended from a teardrop-shaped unipolar or bipolar cell body (Figs. 22, 25, 29). They were usually found in loose aggregates along with sensory cells, with unipolar or flask-shaped interneurons being the most numerous (Fig. 25). The soma of interneurons ranged from 3–5 μm in diameter, which is the size range of the neuronal soma identified *in situ*. In sectional profile, both *in situ* and isolated neurons possessed long slender neurites that emerge from a bulbous base containing the nucleus (Figs. 21, 24, 26). The nucleus was spherical to cuboidal in form and embedded, along with a few mitochondria, in a finely granular cytoplasm (Figs. 22–25). Neurites contained microtubules and a small number of vesicles ranging from 50 to 80 nm in diameter (Figs. 24, 26). All the above features are identical to those of neurons *in situ* in the anterolateral ganglia of the veliger (Chia and Koss, 1989). No synaptic profiles were observed within the ganglion, although synapses were observed in the connectives that connect to the cerebral ganglion. Similarly, synapses were never observed in dissociated cells, and it was not possible to classify them as motoneurons or interneurons.

The cell bodies of sensory cells *in situ* are located within the ganglion along the lateral margin that borders the epidermis (Figs. 5, 27). They are spindle-shaped, and consist of a lightly staining nucleus, free ribosomes, microtubules, and numerous vesicles, all of which are embedded in a relatively clear cytoplasm (Fig. 27). Axonal processes, which project to the neuropil, contain microtubules, vesicles, and the occasional mitochondrion. The characteristic features of sensory neurons include: (1) dendritic processes that are thicker than axons, (2) dendrites that extend from the cell body through the epidermis to terminate externally as a single cilium. The cilium was observed to possess a basal body but no rootlet, (3) large (0.5 μm) electron-dense granules, and (4) numerous vesicles in the cell body. Their dendrites also contain mitochondria and microtubules. The overall appearance (Chia and Koss, 1989) of these cells is retained following dissociation and plating in the culture dishes (Figs. 27, 29, 30). Isolated sensory neurons were recognizable at the level of light microscopy by their characteristic spindle to cigar shape: one of the two processes that radiated out from the soma was thicker, and often shorter, and presumably represented the dendrite (Fig. 29). The nucleus occupied a central location within the cell (Fig. 29). At the fine structural level, the integrity of the sensory cells also remained unchanged. These cells are characterized by a relatively clear, lightly staining cytoplasm that contains free ribosomes and an elliptical to spherical nucleus (Figs. 27, 28, 30). The nucleus is relatively lightly staining, and the axon and dendritic processes can be recognized. The dendrite possesses a single cilium and mitochondria, is generally wider than the axon, and characteristically contains vesicles and electron-dense granules averaging 0.5 μm in diameter (Figs. 27, 28, 30). The cilium lacks a ciliary rootlet as compared to cilia of general ciliated epidermal cells which have rootlets (Fig. 30). However, the cilium could not always be found in all cells suspected of being sensory cells, possibly because this organelle may sometimes have been reabsorbed or truncated after the dissociation. The axons contain microtubules and vesicles and are similar in appearance to the neurites of interneurons described above.

The diagnostic features of the different cell-types found in intact ganglia and in cultures of dissociated ganglia are summarized in Table I.

Figure 8. Section through an isolated microvillus cell, under *in vitro* conditions, showing microvilli (arrows) electron-dense granules (G) and nucleus (NU). Bar = 1 μm.

Figure 9. *In situ* ciliated epidermal cell showing multiple cilia (C) and a densely staining nucleus (NU). Bar = 1 μm.

Figure 10. Phase-contrast photomicrograph of a cultured ciliated epidermal cell showing multiple cilia (C). Bar = 10 μm.

Figure 11. *In vitro* ciliated cell showing multiple cilia (C) and nucleus (NU). Bar = 1 μm.

Figure 12. *In situ* muscle cell showing nucleus (NU) and myofilaments (MF). Bar = 1 μm.

Figure 13. Phase-contrast photomicrograph of an isolated, cultured muscle cell. Bar = 5 μm.

Figure 14. *In vitro* muscle cell showing myofilaments (MF) and nucleus (NU). Bar = 1 μm.

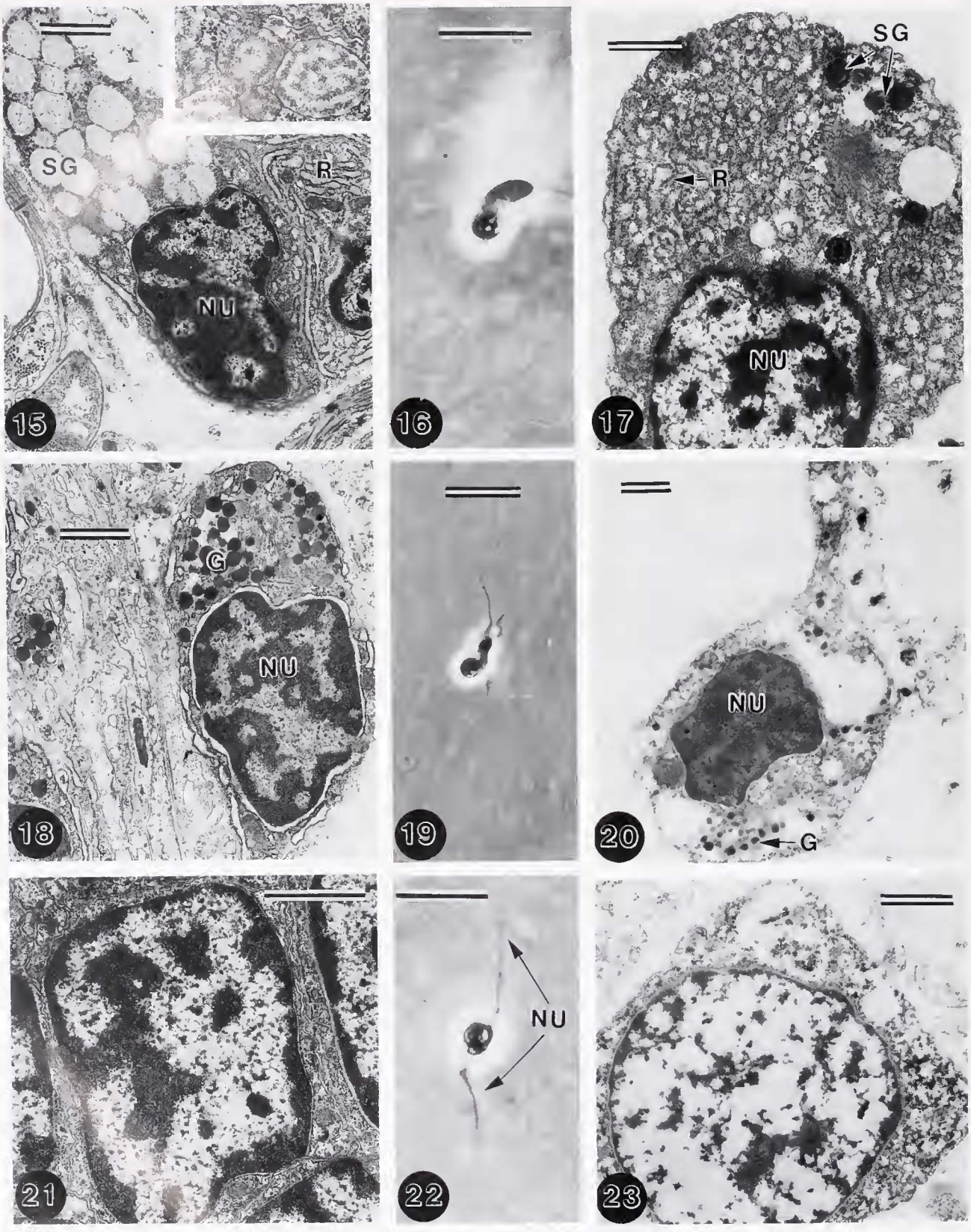

Figure 15. Type A gland cells of an *in situ* metapodial gland showing secretory granules (SG) filled with flocculent material, rough endoplasmic reticulum (R), and a nucleus. Bar = 1 μm. Inset: higher magnification of secretory granules.

Figure 16. Phase-contrast photomicrograph of an isolated, cultured gland cell. Bar = 10 μm.

Table I

Identifying characteristics of cell-types from the anterolateral ganglionic region of Onchidoris bilamellata

Cell-type	Form (*LM and TEM profile)	Staining properties	Size (largest dimension)	Characteristic inclusions and organelles
Metapodial gland cell A	club	lightly granular	10–15 μm	large granules containing flocculent material; rough endoplasmic reticulum
Metapodial gland cell B	flask	densely granular	15 μm	electron-dense granules (0.1 μm diameter)
Muscle cell	thread	densely granular	20–50 μm	myofilaments
Epidermal ciliated cell	cube	densely granular	5–10 μm	multiple cilia; numerous mitochondria
Epidermal microvillus cell	cube	lightly granular	5–10 μm	microvilli; opaque granules (0.2 μm diameter)
Sensory neuron	spindle; one end thicker and often shorter	lightly granular	7–10 μm	single cilium; microtubules; clustered vesicles (0.05–0.08 μm diameter); opaque granules 0.5 μm diameter
Neuron	oval bipolar or unipolar; long slender neurites	lightly granular	10–15 μm	microtubules; few vesicles (0.05–0.08 μm diameter)

* LM = light microscopy; TEM = transmission electron microscopy.
Listed features are shared between identical cell-types found under *in situ* and *in vitro* conditions.

Discussion

Assays that measure whole-organism responses are useful in identifying substances that induce larval settlement and metamorphosis. However, they provide little information about the cellular mechanisms that they activate, or the location (*i.e.,* the structural site) at which they are detected (reviewed by Pawlik, 1990). Therefore, techniques must be developed which enable the study of the precise actions of settlement and metamorphic inducers.

There is considerable evidence suggesting that the induction of settlement and metamorphosis of larval mollusks is mediated by the nervous system (Hadfield, 1978); at the primary level, the process of perceiving natural or artificial inductive substances is ascribed to an external epidermal sensory cell (Baloun and Morse, 1984; Burke, 1983; Morse and Baxter, 1989; Morse, 1990; Trapido-Rosenthal and Morse, 1986; Yool *et al.,* 1986). Receptor cells for these responses in different species of veligers have been localized to the cephalic sensory organ (Bonar, 1978; Morse *et al.,* 1980; Chia and Koss, 1984), rhinophores (Chia and Koss, 1982), and the anterior portion of the foot or propodium (Chia and Koss, 1989). Although the receptive capacities of most of these organs have been inferred from morphological characteristics and relationships, there is little evidence to suggest that all these structures are predisposed to perceive settlement or metamorphic cues. To date, the *Onchidoris* larval foot, or specifically the anterolateral propodial ganglia, represents the only system where morphologically identified chemosensory receptor cells have been shown electrophysiologically to respond to a known settlement cue (Arkett *et al.,* 1989).

In this study we have developed a method for dissociating, isolating, and maintaining the cells that constitute the anterolateral portion of the *Onchidoris* foot, including the sensory neurons and interneurons of the anterolateral ganglia. This technique produces cultures of individual cells, permitting future studies of the cellular mechanisms involved in the detection and transduction of settlement cues; previous studies have been restricted by *in situ* preparations.

This *in vitro* system is unique among preparations for studying veliger settlement because it can be used to study

Figure 17. *In vitro* gland cell showing secretory granules (SG), rough endoplasmic reticulum (R), and nucleus (N). Bar = 1 μm.

Figure 18. Type B secretory cell showing a densely staining nucleus (N) and small electron-dense granules (G). Bar = 1 μm.

Figure 19. Phase-contrast photomicrograph of an isolated, cultured type B gland cell. Bar = 10 μm.

Figure 20. *In vitro* type B gland cell showing small electron-dense granules and a densely staining nucleus. Bar = 1 μm.

Figure 21. Interneuron located in anterolateral ganglion. Bar = 1 μm.

Figure 22. Phase-contrast photomicrograph of a interneuron isolated from the anterolateral ganglion. Note the bipolar shape with neurites (NU) radiating out from the cell body. Bar = 5 μm.

Figure 23. Section through an interneuron under *in vitro* conditions. Bar = 1 μm.

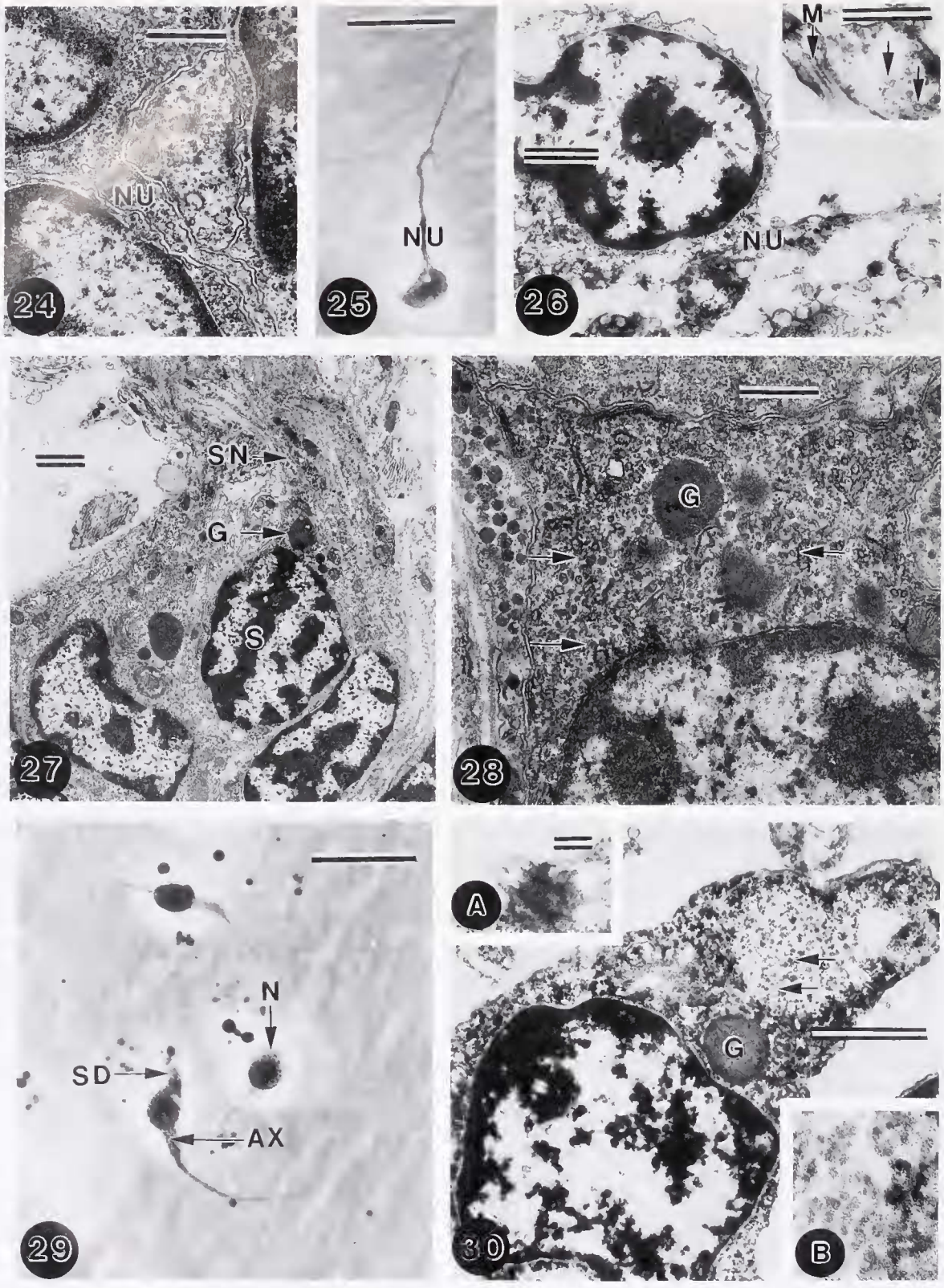

Figure 24. Neurite (NU) of interneuron in an anterolateral ganglion showing vesicles and microtubules. Bar = 1 μm.

Figure 25. Phase-contrast photomicrograph of an isolated interneuron showing a unipolar shape with a single neurite (NU) radiating from the cell body. Bar = 5 μm.

Figure 26. Section through an isolated and cultured interneuron showing a neurite (NU) extending out from the cell body. Inset: neurite with vesicles (arrows) and microtubules. Bars = 0.5 μm.

the immunocytological properties of different cell types, their passive and active electrical properties, and their responses to bioactive substances such as neurotransmitters and neuromodulators. A similar approach has been successfully employed to study the same parameters in neurons dissociated from embryos of the pulmonate, *Helisoma trivolvis* (Goldberg *et al.*, 1988; Goldberg and Price, 1991; Goldberg *et al.*, 1991).

For the most part, the isolated cells retained their basic *in situ* appearance, and could thus be classified according to cell-type by light microscopy. Such classifications were usually confirmed by electron microscopy. There were instances, however, where the appearances of different cell-types overlapped sufficiently to preclude their classification. For instance, the apical ends of many putative sensory cells apparently became rounded following isolation, making them indistinguishable from gland cells. Nevertheless, future studies that combine electrophysiological techniques with those employed here, will ensure accurate diagnosis of each cell-type.

Arkett *et al.* (1989) have demonstrated that settlement receptor cells in *Onchidoris* depolarize in response to a known settlement cue. It is our intention to use the culture system developed in the present study to cultivate the sensory cells and neurons of the anterolateral ganglion for the purpose of voltage- and current-clamping experiments. The electrophysiological effects of settlement inducing-ligands and neurotransmitters can then be directly and precisely monitored on single identified cells. The possible roles of second messengers in mediating settlement and metamorphic responses can then be accurately elucidated.

Acknowledgments

The collection of egg masses, by Dr. A. Martel and M. Sewell, was greatly appreciated. We also wish to thank Dr. D. A. Craig and G. D. Braybrooke for providing Scanning Electron Microscope Facilities, and Dr. S. K. Malhotra for providing Transmission Electron Microscope Facilities. F.-S. C. was supported by NSERC grant #6083 and J.I.G. was supported by NSERC grant #U0553 and the Alberta Heritage Foundation for Medical Research.

Literature Cited

Arkett, S. A., G. O. Mackie, and C. L. Singla. 1987. Neuronal control of ciliary locomotion in a gastropod veliger (*Calliostoma*). *Biol. Bull.* **173:** 513–526.

Arkett, S. A., F.-S. Chia, J. I. Goldberg, and R. Koss. 1989. Identified settlement receptor cells in a nudibranch veliger respond to specific cue. *Biol. Bull.* **176:** 155–160.

Baloun, A. J., and D. E. Morse. 1984. Ionic control of metamorphosis in larval *Haliotis rufescens* (Gastropoda). *Biol. Bull.* **167:** 124–138.

Bonar, D. B. 1978. Ultrastructure of a cephalic sensory organ in larvae of the gastropod *Phestilla sibogae* (Aoelidacea, Nudibranchia). *Tissue Cell* **10:** 153–165.

Burke, R. B. 1983. The induction of metamorphosis of marine invertebrate larvae: stimulus and response. *Can. J. Zool.* **16:** 1701–1719.

Chia, F.-S., and R. Koss. 1982. Fine structure of the larval rhinophores of the nudibranch, *Rostanga pulchra*, with emphasis on the sensory receptor cells. *Cell Tiss. Res.* **225:** 235–248.

Chia, F.-S., and R. Koss. 1984. Fine structure of the cephalic sensory organ in the larva of the nudibranch *Rostanga pulchra* (Mollusca, Opisthobranchia, Nudibranchia). *Zoomorphology* **104:** 131–139.

Chia, F.-S., and R. Koss. 1988. Induction of settlement and metamorphosis of the veliger larva of the nudibranch, *Onchidoris bilamellata*. *Int. J. Invert. Reprod.* **14:** 53–70.

Chia, F.-S., and R. Koss. 1989. The fine structure of the newly discovered propodial ganglia of the veliger larva of the nudibranch, *Onchidoris bilamellata*. *Cell Tiss. Res.* **256:** 17–26.

Goldberg, J. I., D. P. McCobb, P. B. Guthrie, R. A. Lawton, R. E. Lee, and S. B. Kater. 1988. Characterization of cultured embryonic neurons from the snail *Helisoma*. Pp. 85–108 in *Cell Culture Approaches to Invertebrate Neuroscience*, D. J. Beadle, G. Lees, and S. B. Kater, eds. Academic Press, London.

Goldberg, J. I., and C. J. Price. 1991. Voltage-gated ionic currents in neurons isolated from *Helisoma trivolvis* embryos. In *Molluscan Neurobiology*, K. S. Kits, H. H. Boer, and J. Josse, eds. North Holland Publishing Co., Amsterdam (in press).

Goldberg, J. I., L. R. Mills, and S. B. Kater. 1991. Novel effects of serotonin on neurite outgrowth in neurons cultured from embryos of *Helisoma trivolvis*. *J. Neurobiol.* **22:** 182–194.

Hadfield, M. G. 1978. Metamorphosis in marine molluscan larvae: an analysis of stimulus and response. Pp. 165–175 in *Settlement and Metamorphosis of Marine Invertebrate Larvae*, F.-S. Chia and M. E. Rice, eds. Elsevier, New York.

McEuen, F. S. 1985. Reproductive patterns in holothuroids. Ph.D Thesis, The University of Alberta, Edmonton, Canada.

Morse, D. E. 1990. Recent progress in larval settlement: closing the gap between molecular biology and ecology. *Bull. Mar. Sci.* **46**(2): 465–483.

Figure 27. Anterolateral ganglion showing sensory neurons (S) with large electron-dense granules (G) and dendrites (SN) projecting into the epidermis. Bar = 1 μm.

Figure 28. Higher magnification of an *in situ* sensory neuron showing characteristic electron-dense granules (G) interspersed with vesicles (arrows). Bar = 0.5 μm.

Figure 29. Phase-contrast photomicrograph showing an interneuron (N) and a sensory neuron with a shortened dendritic portion (SD) and a thinner axonal segment (AX). Note a second unlabelled sensory cell with a thickened dendritic region. Bar = 5 μm.

Figure 30. Section through a sensory neuron under *in vitro* conditions, showing electron-dense granule (G) and region of vesicles (arrows). Insets: A. Cilium from a dendrite of a sensory neuron. B. Higher magnification of region with vesicles. Bars = 0.5 μm.

Morse, D. E., and G. Baxter. 1989. *In vitro* dissection of chemosensory pathways controlling larval metamorphosis. *Am. Zool.* **29:** 30A.

Morse, D. E., H. Duncan, N. Hooker, A. Baloun, and G. Young. 1980. GABA induces behavioral and developmental metamorphosis in planktonic molluscan larvae. *Fed. Proc.* **39:** 3237–3241.

Pawlik, J. R. 1990. Natural and artificial induction of metamorphosis of *Phragmatopoma lapidosa californica* (Polychaeta: Sabellariidae), with a critical look at the effects of bioactive compounds on marine invertebrate larvae. *Bull. Mar. Sci.* **46**(2): 512–536.

Richardson, K. C., L. Jarrett, and E. H. Finke. 1960. Embedding in epoxy resins for ultrathin sectioning in electron microscopy. *Stain Technol.* **35:** 313–323.

Schacher, S., and E. Proshansky. 1983. Neurite regeneration by *Aplysia* neurons in dissociated cell culture: modulation by *Aplysia* hemolymph and the presence of the initial axonal segment. *J. Neurosci.* **10:** 2403–2413.

Trapido-Rosenthal, H. G., and D. E. Morse. 1986. Availability of chemosensory receptors is down-regulated by habituation of larvae to a morphogenetic signal. *Proc. Natl. Acad. Sci. USA* **83:** 7658–7662.

Wood, R. L., and J. H. Luft. 1965. The influence of buffer systems on fixation with osmium tetroxide. *J. Ultrastruct. Res.* **12:** 22–45.

Yool, A. J., S. M. Grau, M. G. Hadfield, R. A. Jensen, D. A. Markell, and D. E. Morse. 1986. Excess potassium induces larval metamorphosis in four marine invertebrate species. *Biol. Bull.* **170:** 255–266.